

Progress in understanding the multiscale analysis of Magnetic Island interacting with Turbulence in Tokamak

O. Agullo¹, M. Muraglia¹, T. Voslion¹, Z.O. Guimaraes-Filho¹, S. Benkadda¹, P. Beyer¹, I.L. Caldas², X. Garbet³, Yu.K. Kuznetsov², I.C. Nascimento², A. Sen⁴, M. Yagi^{5,6}, F. L. Waelbroeck⁷

¹ *International Institute for Fusion Science, CNRS-Universite de Provence, France*

² *Institute of Physics, University of Sao Paulo, Brazil*

³ *CEA, IRFM, F-13108 Saint Paul Lez Durance, France*

⁴ *Institute for Plasma Research, Bhat, Gandinhagar 382428, India*

⁵ *RIAM, Kyushu University, Japan*

⁶ *Japan Atomic Energy Agency, Japan*

⁷ *Institute for Fusion Studies, University of Texas, Austin, USA*

Abstract. In this paper, we report on progress in understanding the multiscale dynamics of magnetic islands in presence of turbulence. We focus numerically on two different kinds of small-scales turbulence, namely, pressure and flow driven turbulences. Experimentally, using TCABR tokamak experimental data, we also show a complex coexistence of turbulent electrostatic and magnetic fluctuations and the effect of edge biasing on the growth of magnetic instabilities.

1. Introduction

In fusion devices small scale instabilities can generate small-scales turbulence. Several experiments report the coexistence of both microturbulence and MHD activities[1, 2]. However, the mechanisms involving the coexistence of turbulence and magnetic islands is still not well understood. In this paper, we show that the interaction of turbulent structures with magnetic islands can be sustained by different types of mechanisms which depends on the equilibrium configurations and/or the experimental situations. In particular, we focus on the impact of the turbulence on the nonlinear dynamics of magnetic islands using a 2D reduced two-fluid model in a slab geometry. In a first part, we investigate how the interchange turbulence affects nonlinearly the formation of a magnetic island. We find that small-scales interchange turbulence which develops in the vicinity of the resonance perturbs and enhances magnetic island formation thanks to nonlinear beating of the small-scales interchange modes and cascade phenomena. In a second part, we study the effect of Kelvin-Helmoltz instability (KHI) on a double tearing mode. Flow gradients in the shear layer can generate island rotation, instabilities and turbulence. In this case, the turbulence is generated outside the resonant surfaces and takes place in between the two magnetic islands. Mechanisms such that turbulence spreading into the island and force reconnection modify strongly the dynamics leading to a global reconnection of the double tearing mode structure. Finally, an analysis of a TCABR Tokamak experimental data show that edge biasing can have very different effects on the evolution of the magnetic activity intensity. The latter can grows affecting the edge turbulence in two different operational regimes found in TCABR: in one of them the edge biasing suppresses the growth of the magnetic activity, while in the other one the edge biasing excites the magnetic instability. The growth of the magnetic activity was found linked to the interaction of 3/1 and 2/1 modes and in the biasing excitation regime, the latter dominates.

2. Impact of turbulence on nonlinear formation and dynamics of an island

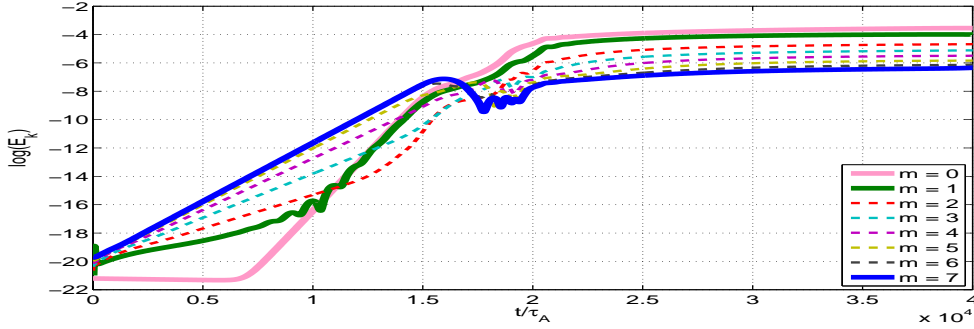


Figure 1: Time evolution of the kinetic energy for the modes $0 \leq m \leq 7$, $\Delta' = 2$.

In this section, we study the interaction of a magnetic island with small scale turbulence [3, 4]. More precisely, we focus on the effect of interchange small-scales turbulence on the dynamics of a magnetic island driven by a tearing instability. Like in [5], we consider a two-dimensional plasma model based on the two fluid Braginskii equations in the drift approximation [6] with cold ions and isothermal electrons. Typically, it involves a set of coupled equations for the electrostatic potential ϕ , the electronic pressure p and the magnetic flux ψ :

$$\frac{\partial}{\partial t} \nabla_{\perp}^2 \phi + \{\phi, \nabla_{\perp}^2 \phi\} = \{\psi, \nabla_{\perp}^2 \psi\} - \kappa_1 \frac{\partial p}{\partial y} + \mu \nabla_{\perp}^4 \phi, \quad (1)$$

$$\frac{\partial}{\partial t} p + \{\phi, p\} = -v_{\star} \left((1 - \kappa_2) \frac{\partial \phi}{\partial y} + \kappa_2 \frac{\partial p}{\partial y} \right) + \hat{\rho}^2 \{\psi, \nabla_{\perp}^2 \psi\} + \chi_{\perp} \nabla_{\perp}^2 p, \quad (2)$$

$$\frac{\partial}{\partial t} \psi = \{\psi, \phi - p\} - v_{\star} \frac{\partial \psi}{\partial y} + \eta \nabla_{\perp}^2 \psi \quad (3)$$

The equilibrium quantities are a constant pressure gradient and a magnetic field corresponding to a Harris current sheet model [7]. Equations (1-3) are normalized using the characteristic Alfvén speed v_A and the magnetic shear length L_{\perp} . Further, $\kappa_1 \sim \frac{L_{\perp}}{R_0}$ and $\kappa_2 \sim \frac{L_p}{R_0}$ are the curvature terms with R_0 representing the major radius of a toroidal plasma configuration. L_p is the gradient scale length, τ_A is the Alfvén time based on reference length scale L_{\perp} . μ is the viscosity, χ_{\perp} the perpendicular diffusivity, η is the plasma resistivity. v_{\star} and $\hat{\rho}$ are the normalized electron diamagnetic drift velocity and ion sound Larmor radius. In order to understand how the interchange mechanism affects the formation of a magnetic island, we have performed linear and nonlinear simulations of the equation (1-3). A semispectral code with a 2/3 dealiasing rule in the poloidal direction, a resolution of 256 grid points in the radial direction, 64 poloidal modes has been used. The computational box size is $L_x = 2\pi$ and $L_y = 5\pi$. In this study we have fixed $\hat{\rho} = 0.04$, $v_{\star} = 10^{-2}$, $\kappa_2 = 0.36$ and the dissipative parameters (μ , χ_{\perp} , η) are taken to be equal at 10^{-4} . When the aspect ratio L_y/L_x is large enough, the poloidal tearing mode $m=1$ ($k_m = m2\pi/L_y$) becomes unstable which corresponds to a positive value of the tearing stability index Δ' . In this work, the equilibria are such that tearing modes $m > 1$ are linearly stable. To characterize how the interchange small-scales acts on the formation of a magnetic island, we will analyze linear and nonlinear simulations with different values of Δ' . Interchange parameter κ_1 is set equal to 5 which implies that some of the modes $m > 1$ are unstable with respect to interchange instability, despite the stabilizing role of the equilibrium magnetic field. The latter situation, where interchange is stable, was studied in [5]. In this work, the most unstable interchange mode is held fixed to $m = 7$.

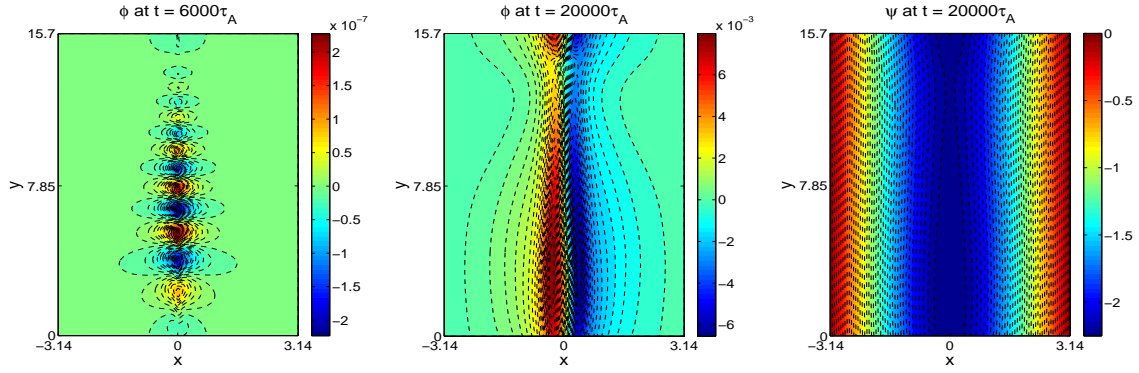


Figure 2: Snapshots of the electrostatic potential ϕ and the magnetic flux ψ , $\Delta' = 2$.

Fig.1 presents the time evolution of the kinetic energy of the modes $0 \leq m \leq 7$ for a nonlinear simulation with $\Delta' = 2$. We observe that the dynamics presents 3 main regimes. During the first phase, $0 < t/\tau_A < 6500$, the dynamics is fully linear. Interchange instability is present at small-scales, dominates energetically and we observe a slow growth of the mode $m = 1$ which is a tearing mode, *i.e.* it presents a tearing parity (ψ even, ϕ and p odd with respect with the resonant surface $x = 0$), while for $m > 1$ interchange parity is observed (ψ odd, ϕ and p even). The mode $m = 0$ is not generated. The interchange structure of the most unstable mode $m = 7$ is clearly observed on snapshots during this phase and, as an illustration, is shown on the left graph of fig. 2. Note that the mode structure is localized in the vicinity of the resistive layer. During the second phase or regime, from $t = 6500\tau_A$ where the mode $m = 0$ starts to be generated to $t = 16450\tau_A$ where the mode $m = 7$ reaches a maximum, the dynamics becomes fully nonlinear. Mainly, in this phase the interaction of the interchange small-scales affects the large scales $m = 0$ and $m = 1$. Fig. 1 shows that the growth rate of mode $m = 0$, γ_0^{nl} , is twice the one of $m = 7$ as the result of a beating of two interchange modes which, by nonlinear interactions, produce modes with tearing parity. The same picture occurs for mode $m = 1$ because $\gamma_1 \sim \gamma_6 + \gamma_7 \sim \gamma_0$. The beating of modes $m = 7$ and $m = 6$ as well as modes $m = 1$ and $m = 0$ enhances the growth of the tearing mode $m = 1$.

The last regime begins when the tearing modes $m = 0$ and $m = 1$ become the most dominant modes, at $t = 16450\tau_A$. Fig.1 shows that during this regime the energy of the interchange small-scale decreases quickly. A analysis of the eigenfunctions shows that after $t = 16450\tau_A$ the interchange modes ($m > 1$) loose the interchange parity and get that of the tearing. In fact a direct cascade of the tearing mode $m = 1$ allows the generation of $m = 2$ tearing mode which gets the tearing parity (the nonlinear interaction of tearing modes conserves tearing parity). In fig. 2 are shown the snapshots of ϕ and ψ during the last regime at $t = 20000\tau_A$. Large scale tearing parity dominates and a magnetic island is observed. In this case, and more generally when $\Delta' > 0$, there are two sources leading to the generation of a magnetic island, the large scale tearing instability and the small scale interchange instability. We find also that the resulting nonlinear structure of the mode depends on the nature of the source. Indeed, the snapshots reveal that the classical picture resulting from tearing instability theory is not universal: We observe that the magnetic island is not maintained by a quadrupole flow structure, which would be the case in the absence of interchange instability. The flow surrounding the magnetic island present in fact a dipole structure in terms of electrostatic potential, the flow going in and out in the vicinity of the x-point.

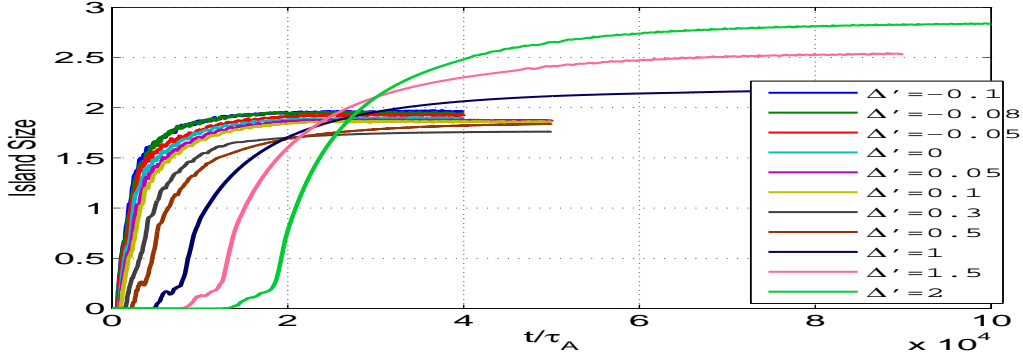


Figure 3: time evolution the island size for nonlinear simulations for different values of Δ'

The previous paragraphs show that tearing instability is not required to generate magnetic island and it is interesting to see if the small scale turbulence can originate small seed islands which are important in the context of neoclassical tearing modes [8]. We have performed the same simulations except we have modified the equilibrium profile, taking different values of Δ' , in order to study the impact of the tearing instability on the asymptotic size of the islands. In Fig. 3 are plotted the time evolution of the magnetic island size for these different simulations. It shown that even for negative values of Δ' (stable tearing mode), the beating of the interchange modes can produce a magnetic island which grows quickly. When the tearing mode is marginally stable, the saturated island size is small and does not depend on Δ' .

3. Global reconnection of the double tearing mode in presence of a shear flow

We focus here on how the presence of a shear flow in between two resonant surfaces - which have been observed experimentally [9] - influences the nonlinear global reconnection process of the double tearing mode (DTM). Compared with previous section, curvature, diamagnetic and pressure effects are switched off but an equilibrium shear flow is introduced into the dynamics. In this work, the islands are close enough to finally trigger off a global reconnection whatever the importance of the imposed shear flow and $v_{s.f.} < 0.3v_A$. $v_{s.f.}$ is maximal velocity of the shear flow and roughly the imposed plasma flow velocity in the vicinity of the resonant surfaces. Their distance is of the order of the characteristic magnetic shear length L_\perp . In the limit of weak flow compared to Alfvén velocity, which corresponds to experimental observations, the flow gradient acts as a weak external forcing which perturbs the DTM growth. Gradients of velocity in reversed shear plasmas are usually located in between resonant surfaces [9, 10]. In contrast to the DTM structure obtained without forcing, the shear flow tends to push the islands growing on the resonant surfaces ($x = \pm x_r$) in opposite poloidal directions. The resulting flow pattern presents a symmetry breaking with respect to $x = 0$ surface. It can be shown that it originates the generation of a zonal flow ($m = 0$ mode) which impacts on the nonlinear dynamics of DTM [11].

Let us first focus on the impact of some important parameters on the linear dynamics. Previous works focused on the role of the core rotation parameter [12]. Figure 4 shows the linear growth rate of the double tearing poloidal mode $m = 1$ as a function of the resistivity in presence of a weak shear flow ($v_{s.f.} = 3\%v_A$). At high resistivity, $\eta > 2.10^{-4}$, the magnetic structures grow in the vicinity on the resonant surfaces and impose, both, a flow and a magnetic field in between the resonant surface which inhibits the island rotations despite the presence of the

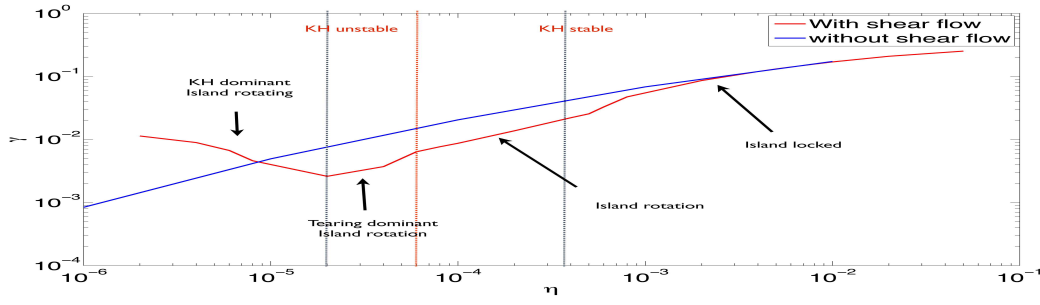


Figure 4: Growth rate of poloidal mode $m = 1$ as a function of resistivity

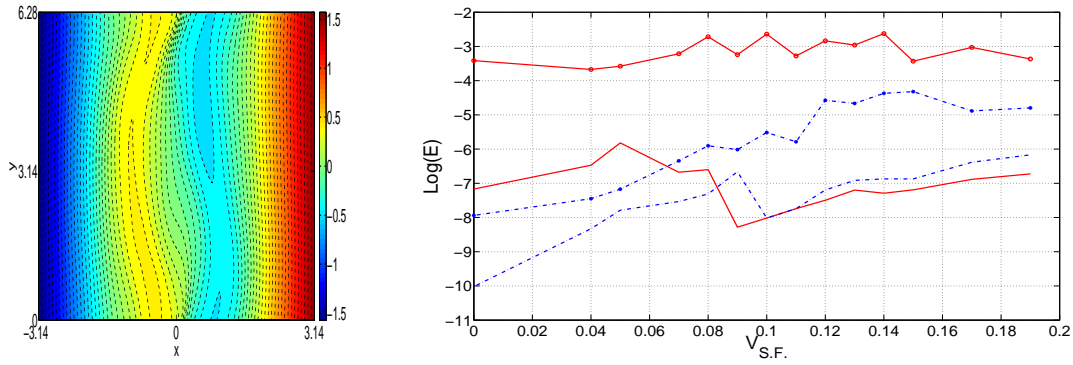


Figure 5: Left: Magnetic flux in nonlinear regime. $v_{s.f.} = 0.15$, $\eta = \nu = 10^{-4}$. Right: Kinetic energy (dashed blue), and magnetic energy (red) as a function of the shear flow amplitude $v_{s.f.}$. [Undotted] When kinetic energy reaches a first maximum. [Dotted] Just before global reconnection mechanism occurs.

shear flow. For $\eta \in [7 \cdot 10^{-5}, 2 \cdot 10^{-4}]$, the interactions between resonant surfaces is weakened and magnetic island rotations develop. In the interval of resistivity $2 \cdot 10^{-5} < \eta < 7 \cdot 10^{-5}$, KHI is observed at wave number $m > 1$: Weak vortices appear in the shear layer and the maximum growth rate occurs typically at $m = 5$. This wave number depends of course on the level of the shear localized in the vicinity of $x = 0$ but the higher the latter is, the higher the dominant wave number is. In this resistive parameter range, the growth rate of the DTM is higher than the KH's one. First, let us emphasize that, linearly, the tearing mode structure generates a flow which links the two magnetic island and inhibit or weaken, both, the island poloidal rotations and the KHI in the shear layer. Increasing the resistivity value strengthens the tearing instability and kills KHI. Second, lowering the resistivity value weakens the flow linking the magnetic structures of the DTM. As a result the growth rate of the tearing mode $m = 1$ is reduced compare with the case without shear flow, as can be seen in figure (4). At low resistivity $\eta < 2 \cdot 10^{-5}$, the growth rate of $m = 1$ is enhanced due to the development of large scale KHI in between the two resonance surfaces.

In the limit of low resistivity, KHI can lead to the generation of a turbulent state resulting from the interplay between DTM and multi-scale Kelvin-Helmoltz dynamics. In fact, both, low resistivity and high shear flow amplitude leads to KH instability and nonlinear turbulent states which can affect strongly the magnetic island dynamics. To illustrate this point, in figure 5, a snapshot of the magnetic flux in the nonlinear phase for $v_{s.f.} = 0.15$, $\eta = \nu = 10^{-4}$ and a

distance between the islands $\delta_{x_r} = \pi/2[L_\perp]$ is shown. It appears that the islands are strongly shaken and are not localized and/or align along the resonant surfaces. This unusual behavior is linked to the generation of a high level of kinetic energy which requires some further analyses.

The role of the kinetic energy in the nonlinear dynamics of the islands can be studied by looking at its level for different values of $v_{s.f.}$. This is presented in figure (5). The undotted curves gives the energy level of, both, the kinetic energy (blue) and magnetic (red) energies when the system reaches a first saturation from a kinetic point of view. Note that between $v_{s.f.} = 0.09$ and $v_{s.f.} = 0.1$, the kinetic level strongly decreases. This is due to the fact that KHI gets a growth rate higher than the DTM's one and in the latter case saturation occurs with a lower level of both kinetic and magnetic energy. The graph shows also clearly that kinetic energy becomes higher than magnetic energy as might be expected from a KH like instability. Note that the decreases of the magnetic energy starts as far as KHI becomes unstable, *i.e.* $v_{s.f.} > 0.05$, and is linked to the fact that, both the island rotation and KH vortices weaken the interaction between the two resonant surface. This situation presents some similarity with a wall-island interaction which can also stabilize a resistive instability [14].

Figure (5) shows the kinetic and magnetic energy levels just before global magnetic reconnection occurs. Note that during the nonlinear phase a flow is generated in the vicinity of resonant surfaces, stopping islands rotations, which is required for global reconnection process to start [11]. The graph shows, first, the magnetic energy fluctuations require for global reconnection process to occurs does not depend on the shear flow amplitude. Second, the kinetic energy growth roughly exponentially with $v_{s.f.}$ in the range where KHI ($m > 1$) is unstable but with a lower growth rate than $m = 1$ DTM. The magnetic island appear to be localized on the magnetic surfaces in that phase, despite an enhancement of the spreading of kinetic energy into the island (E_k/E_m has an exponential growth). Third, when $v_{s.f.} \geq 0.12$, *i.e.* the growth of mode $m = 1$ is dominated by KHI, it saturates. In this latter case, the system shows strong spatial kinetic fluctuations and is in a turbulent state. The island are also strongly shaken (see figure 5). However global reconnection mechanism occurs earlier and explain partially that kinetic energy does not increase anymore with $v_{s.f.}$. Another mechanism seems to be at play: Not only the flow generated in the shear layer is incomming into the island (spreading of the turbulence) but also the shear flow layer, by generating large scale vortices in its vicinity, pinches the magnetic surfaces and therefore a forced magnetic reconnection mechanism is at play. Note that, noteworthy in the linear regime, we have seen that the shear flow can stabilize the grow of the DTM. Here the shear flow is doing the opposite by enhancing the magnetic reconnection.

4. Experimental observations of the interplay between turbulence and magnetic islands in TCABR tokamak

TCABR is a small tokamak that operates with Hydrogen plasmas and which main parameters are: central magnetic field $B_0=1.1$ T, major radius $R=0.61$ m, and circular plasma shape defined by a material limiter at $a=0.18$ m [15]. Unlike most tokamaks, in TCABR tokamak the frequency spectra of electrical and magnetic fluctuations have a peculiar partial superposition. Moreover, in some discharges the MHD activity can enhance and modulate the electrostatic turbulence at the edge of the plasma [16], providing experimental observations of coupling and synchronization between magnetic and electrostatic fluctuations [17, 18, 19].

These properties were observed in two operational regimes of TCABR [16]. Accordingly, Fig.

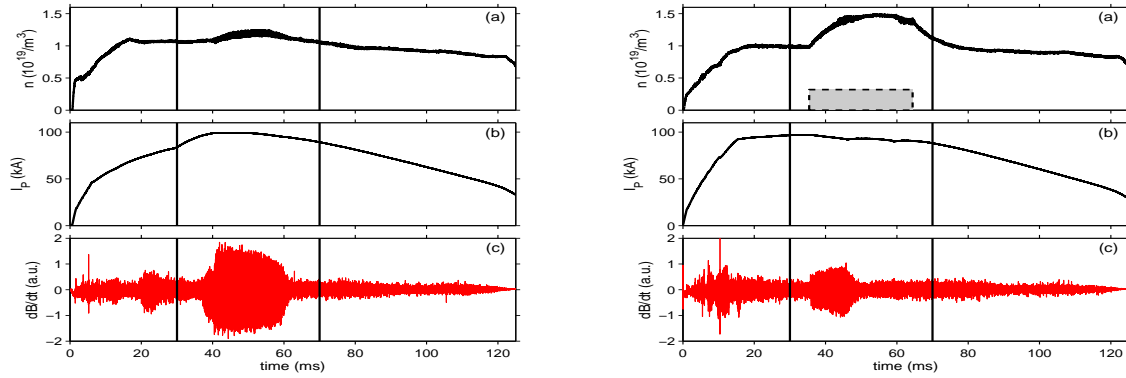


Figure 6: Evolution of the plasma parameters in the two regimes with enhancement of MHD activity in TCABR. (a) is the plasma density, (b) is the plasma current, and (c) is a Mirnov coil signal. [Left] Regime with a natural MHD growth. [Right] Regime with bias excitation. The dashed rectangle indicates the time with biasing.

6 shows the time traces of the plasma discharge in these two regimes with high MHD activity. For the regime presented in the left panel of Fig. 6, the plasma current increases slowly and the MHD activity (measured by Mirnov coils) grows without any external perturbation. In this case the MHD enhancement is observed whenever the edge safety factor approaches an integer number, what could be associated to a MHD instability excitation [20]. On the other hand, for the regime presented in the right panel of Fig. 6, the growth of the MHD activity starts few milliseconds after the edge biasing polarization, performed with an electrode inserted in the plasma edge (at $r/a \sim 0.92$) [21]. It should be noted that the initial effect of the edge biasing is to reduce the turbulence in the edge region, improving the plasma confinement [21, 22]. However, the growth of the MHD activity is frequently observed in this regime. For both regimes, the enhancement of the MHD activity strongly affects the behavior of the plasma edge turbulence, as it can be seen in Fig. 7, which shows the spectrograms of the electrostatic signals (measured by Langmuir probes) and the MHD activity. It is possible to observe that after the growth of the MHD activity, the spectral characteristics of the magnetic oscillations are also observed in the electrostatic turbulence.

The intensity of the modulation of the turbulence by the MHD activity in TCABR was quantified through some methods commonly used for dynamical system characterization. For instance, a modified version of the order parameter was used to quantify the spatial-temporal regularity of the turbulence at the MHD frequency in the bias excitation regime [17]. Moreover, the bispectral analysis was used to determine the radial profile of the turbulence alterations in the regime with natural MHD growth [18]. Furthermore, the Recurrence Quantification Analysis was used to evaluate the profile of the dynamical alterations on turbulence in the regime with natural excitation [19]. While the two spectral based methods show effects concentrated in the edge region, the recurrence based method indicates that the alterations in the dynamic behavior are wide-ranging, and they can be clearly observed in both edge and SOL region.

The alteration of the edge electrostatic potential through the bias polarization has different effects on the two operational regimes: in the regime with natural excitation if the edge biasing is applied before the growth of the MHD activity it can suppress (or to retard) the enhancement of the MHD activity [16]. Moreover, the growth of the MHD activity in the natural excitation regime presents two saturated stages at very different power spectral values of magnetic

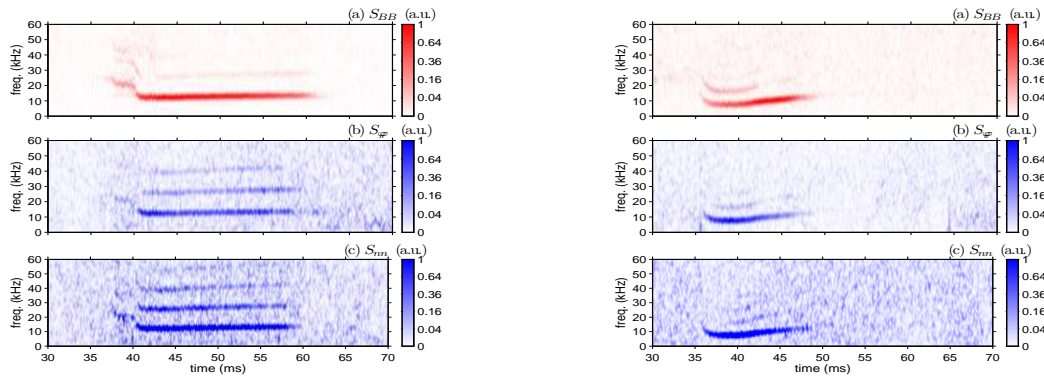


Figure 7: Spectrograms of magnetic and turbulent signals in the time intervals indicated by vertical lines in Fig.6. Spectrograms of the magnetic oscillations (a), the floating potential (b) and the local plasma density (c). [Left] Regime with natural MHD enhancement. [Right] Regime with bias excitation.

activity. The origin of these two saturated states is not so clear, but it may be linked to non-linear coupling between the (m/n) 3/1 and 2/1 modes. It is consistent with the analysis of the magnetic fluctuations that shows the coexistence of these two modes [16]. In fact, it has been observed that the evolution of the intensity of the modes detected on the Mirnov coils signals are not equal in the two regimes. In the natural excitation regime the intensity of these two modes are similar, while in the biasing excitation regime the 2/1 is clearly the strongest mode.

References

- [1] B.J. Ding et al, *Plasma Phys. Control. Fusion* **46**, 1467 (2004)
- [2] K. Tanaka et al, *Nucl. Fusion* **46**, 110 (2005)
- [3] M. Yagi et al, *J. Plasma Fusion Res.* **2**, 025 (2007)
- [4] F. Militello et al, *Phys. Plasmas* **15**, 050701 (2008)
- [5] M. Muraglia et al, *Nucl. Fusion* **49**, 055016 (2009)
- [6] M. Ottaviani et al, *Phys. Rev. Lett.* **93**, 075001 (2004)
- [7] D. Biskamp, *Magnetic Reconnection in Plasmas*, Cambridge University Press (2000)
- [8] O. Sauter et al, *Phys. Plasmas* **4**, 1654 (1997)
- [9] R.C. Wolf, *Plasma Phys. Control. Fusion* **45**, R1–R91 (2003).
- [10] T. Tala, et al, *Nucl. Fusion* **47**, 1012–1023 (2007).
- [11] T. Voslioni et al, *J. Plasma Fusion Res. SERIES*, Vol. 9 (2010).
- [12] A. Bierwage et al, *Physics of plasmas* **14**, 010704 (2007).
- [13] A. Ishizawa et al, *Physics of plasmas* **14**, 040702 (2007)
- [14] M. Takeji, et al, *Nucl. Fusion* **42**, 05 (2002).
- [15] R.M.O. Galvão et al, *Plasma Phys. Controlled Fusion* **43**, 1181 (2001).
- [16] I.C. Nascimento et al, *Nuclear Fusion* **47**, 1750 (2007).
- [17] Z.O. Guimarães-Filho et al, *Phys. of Plasmas* **15**, 062501 (2008).
- [18] G.Z. dos Santos Lima et al, *Phys of Plasmas* **16**, 042508 (2009).
- [19] Z.O. Guimarães-Filho et al, *J. Physics Conf. Series* **260**, 012014 (2010).
- [20] K. Makishima et al, *Phys. Rev. Lett.* **36**, 142 (1976).
- [21] I.C. Nascimento et al, *Nuclear Fusion* **45**, 796 (2005).
- [22] F.A. Marcus et al, *Phys. of Plasmas* **15**, 062501 (2008).